We are IntechOpen,
the world's leading publisher of
Open Access books
Built by scientists, for scientists

6,900
Open access books available

186,000
International authors and editors

200M
Downloads

154
Countries delivered to

Our authors are among the

TOP 1%
most cited scientists

12.2%
Contributors from top 500 universities

BOOK
CITATION
INDEX
CLARIVATE ANALYTICS
INDEXED

WEB OF SCIENCE™

Selection of our books indexed in the Book Citation Index
in Web of Science™ Core Collection (BKCI)

Interested in publishing with us?
Contact book.department@intechopen.com

Magnetite Molybdenum Disulphide Nanofluid of Grade Two: A Generalized Model with Caputo-Fabrizio Derivative

Farhad Ali, Madeha Gohar, Ilyas Khan,
Nadeem Ahmad Sheikh, Syed Aftab Alam Jan and
Muhammad Saqib

Additional information is available at the end of the chapter

Abstract

Heat and mass transfer analysis in magnetite molybdenum disulphide nanofluid of grade two is studied. MoS_2 powder with each particle of nanosize is dissolved in engine oil chosen as base fluid. A generalized form of grade-two model is considered with fractional order derivatives of Caputo and Fabrizio. The fluid over vertically oscillating plate is subjected to isothermal temperate and species concentration. The problem is modeled in terms of partial differential equations with sufficient initial conditions and boundary conditions. Fractional form of Laplace transform is used and exact solutions in closed form are determined for velocity field, temperature and concentration distributions. These solutions are then plotted for embedded parameters and discussed. Results for the physical quantities of interest (skin friction coefficient, Nusselt number and Sherwood number) are computed in tables. Results obtained in this work are compared with some published results from the open literature.

Keywords: Caputo-Fabrizio approach, MHD, nanofluid, generalized second-grade fluid, exact solutions

1. Introduction

The idea of fractional order calculus is as old as traditional order calculus. The pioneering systematic studies are devoted to Riemann-Liouville and Leibniz [1]. The subject is growing day by day and its applications have been utilized in different fields, for example, viscoelasticity, bioengineering, biophysics and mechatronics [2]. The applications of non-integer order calculus have also been encountered in different areas of science despite mathematics and physics drastically [3–5]. In fluid dynamics, the fractional order calculus has been broadly used to describe the viscoelastic behaviour of the material. Viscoelasticity of a material is defined it deforms evince both viscous and elastic behaviour via storage of mechanical energy and simultaneous behaviour. Mainardi [6] examined the connections among fractional calculus, wave motion and viscoelasticity. It is increasingly seen as an efficient tool through which useful generalization of physical concepts can be obtained. Hayat et al. [7] studied the periodic unidirectional flows of a viscoelastic fluid with the Maxwell model (fractional). Qi and Jin [8] analyzed the unsteady rotating flows of viscoelastic fluid with the fractional Maxwell model between coaxial cylinders. Many other researchers used the idea of fractional calculus and published quite number of research papers in some reputable journals [9–11].

Several versions of fractional derivatives are now available in the literature; however, the widely used derivatives are the Riemann-Liouville fractional derivatives and Caputo/fractional derivative [12, 13]. However, the researchers were facing quite number of difficulties in using them. For example, the Riemann-Liouville derivative of a constant is not zero and the Laplace transform of Riemann-Liouville derivative contains terms without physical significance. Though the Caputo fractional derivative has eliminated the short fall of Riemann-Liouville derivative, its kernal has singularity point. Ali et al. [14] reported the conjugate effect of heat and mass transfer on time fraction convective flow of Brinkman type fluid using the Caputo approach. Shahid et al. [15] investigated the approach of Caputo fractional derivatives to study the magnetohyrodynamic (MHD) flow past over an oscillating vertical plate along with heat and mass transfer. Recently, Caputo and Fabrizio (CF) have initiated a fractional derivative with no singular kernel [16]. However, Shah and Khan [17] analyzed that heat transfer analysis in a grade-two fluid over an oscillating vertical plate by using CF derivatives. Ali et al. [18] studied the application of CF derivative to MHD free convection flow of generalized Walter's-B fluid model. Recently, Sheikh et al. [19] applied CF derivatives to MHD flow of a regular second-grade fluid together with radiative heat transfer.

However, the idea of fractional calculus is very new in nanoscience, particularly in nanofluid also called smart fluid [20]. In this study, we have applied the fractional calculus idea more exactly, the idea of CF derivatives to a subclass of differential type fluid known as the second-grade fluid with suspended nanoparticles in spherical shape of molybdenum disulphide (MoS_2). Generally, the purpose of nanoparticles when dropped in regular fluid/base fluid/host fluid is to enhance the thermal conductivity of the host fluid. The inclusion of nanomaterial not only increases the thermal conductivity but also increases the base fluid viscosity (Wu et al. [21], Wang et al. [22], Garg et al. [23] and Lee et al. [24]). For this purpose, several types of nanomaterials, such as carbides, oxides and iron, and so on, are available in the market with their specific usage/characteristics and applications. For example, nanomaterial can be used as a nanolubricants, friction reductant, anti-wear agent and additive to tribological performance.

Oxides, such as copper (CuO_2) and titanium oxides (TiO_2), can be used as an additive to lubricants. The combustion of fossil fuels produces injurious gases (CO and NO) that cause air pollution and global warming. To save natural recourses and produce environment-friendly products, currently, nanomaterials are used to enhance the fuel efficiency of the oils [25].

Among the different types of nanomaterial, there is one called molybdenum disulphide nano-material MoS_2, used very rarely in nanofluid studies. Although MoS_2 nanoparticles are not focused more, they have several interesting and useful applications. Applications of molybde-num disulphide can be seen in MoS_2-based lubricants such as two-stroke engines, for example, motorcycle engines, automotive CV and universal joints, bicycle coaster brakes, bullets and ski waxes [26]. Moreover, the MoS_2 has a very high boiling point and many researchers have investigated it as a lubricant The first theoretical study on MoS_2-based nanofluid was performed by Shafie et al. [27], where they studied the shape effect of MoS_2 nanoparticles of four different shapes (platelet, cylinder, brick and blade) in convective flow of fluid in a channel filled with saturated porous medium.

By keeping in mind the importance of MoS_2 nanoparticles, this chapter studies the joint analysis of heat and mass transfer in magnetite molybdenum disulphide viscoelastic nanofluid of grade two. The concept of fractional calculus has been used in formulating the generalized model of grade-two fluid. MoS_2 nanoparticles of spherical shapes have been used in engine oil chosen as base fluid. The problem is formulated in fractional form and Laplace transform together. CF derivatives have been used for finding the exact solution of the problem. Results are obtained in tabular and graphical forms and discussed for rheolog-ical parameters.

2. Solution of the problem

Let us consider heat and mass transfer analysis in magnetite molybdenum disulphide nanofluid of grade two with viscosity and elasticity effects. MoS_2 nanoparticles in powder form of spherical shape are dissolved in engine oil chosen as base fluid. MoS_2 nanofluid is taken over an infinite plate placed in xy-plane. The plate is chosen in vertical direction along x-axis, and y-axis is transverse to the plate. Electrically conducting fluid in the presence of uniform magnetic B_0 is considered which is taken normal to the flow direction. Magnetic Reynolds number is chosen very small so that induced magnetic field can be neglected. Before the time start, both the fluid and plate are stationary with ambient temperature T_∞ and ambient concentration C_∞. At time $t = 0^+$, both the plate and fluid starts to oscillate in its own direction with constant amplitude U and frequency ω. Schematic diagram is shown in **Figure 1**.

Under these assumptions, the problem is governed by the following system of differential equations:

$$\rho_{nf}\frac{\partial u}{\partial t} = \mu_{nf}\frac{\partial^2 u}{\partial y^2} + \alpha_1\frac{\partial^3 u}{\partial t \partial y^2} - \sigma_{nf}B_0^2 u + g(\rho\beta_T)_{nf}(T - T_\infty) + g(\rho\beta_C)_{nf}(C - C_\infty), \qquad (1)$$

$$(\rho c_p)_{nf}\frac{\partial T}{\partial t} = k_{nf}\frac{\partial^2 T}{\partial y^2}, \qquad (2)$$
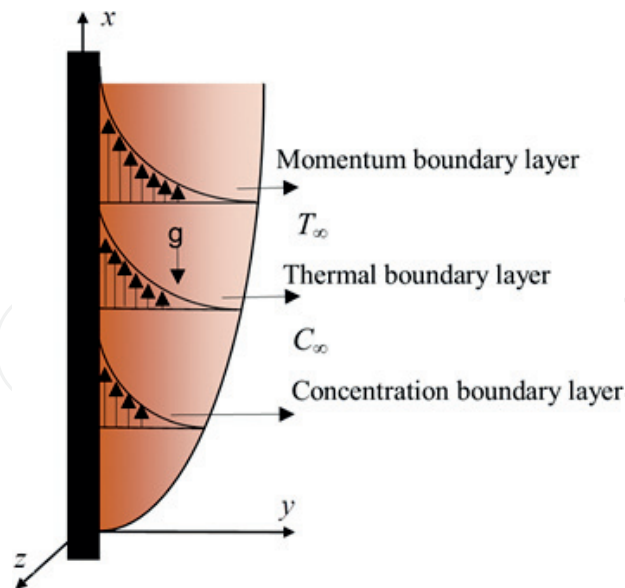
Figure 1. Schematic Diagram of the flow.

$$\frac{\partial C}{\partial t} = D_{nf} \frac{\partial^2 C}{\partial y^2},$$

(3)

where ρ_{nf}, σ_{nf}, μ_{nf} $(\beta_T)_{nf}$, $(\beta_C)_{nf}$, k_{nf}, $(\rho C_p)_{nf}$, D_{nf} are the density, electrical conductivity, viscosity, thermal expansion coefficient, coefficient of concentration, thermal conductivity, heat capacity and mass diffusivity of nanofluid. α_1 shows second two parameters, and g denotes acceleration due to gravity.

The appropriate initial and boundary conditions are

$$
\begin{array}{llll}
u(y,0) = 0 & T(y,0) = T_\infty & C(y,0) = C_\infty & y > 0, \\
u(0,t) = UH(t)\cos\omega t & T(0,t) = T_w & C(0,t) = C_w & t > 0, \\
u(\infty,t) = 0 & T(\infty,t) = T_\infty & C(\infty,t) = C_\infty & \text{as } y \to \infty, \quad t > 0.
\end{array}
$$

(4)

For nanofluids, the expressions for ρ_{nf}, μ_{nf}, $\rho\beta_{nf}$, $(\rho c_p)_{nf}$ are given by:

$$\mu_{nf} = \frac{\mu_f}{(1-\phi)^{2.5}}, \quad \rho_{nf} = (1-\phi)\rho_f + \phi\rho_s, \quad (\rho\beta_T)_{nf} = (1-\phi)(\rho\beta)_f + \phi(\rho\beta)_s,$$

$$(\rho\beta_C)_{nf} = (1-\phi)(\rho\beta)_f + \phi(\rho\beta)_s, \quad (\rho c_p)_{nf} = (1-\phi)(\rho c_p)_f$$

$$+\phi(\rho c_p)_s, \quad \sigma_{nf} = \sigma_f \left(1 + \frac{3(\sigma-1)\phi}{(\sigma+2)-(\sigma-1)\phi}\right),$$

$$\sigma = \frac{\sigma_s}{\sigma_f}, \quad \frac{k_{nf}}{k_f} = \frac{(k_s + 2k_f) - 2\phi(k_f - k_s)}{(k_s + 2k_f) + \phi(k_f - k_s)}, \quad D_{nf} = (1-\phi)D_f.$$

(4a)

Model	$\rho\left(kgm^{-3}\right)$	$C_p\left(Jkg^{-1}K^{-1}\right)$	$C_p\left(Jkg^{-1}K^{-1}\right)$	$\beta \times 10^{-5}\left(K^{-1}\right)$
Engine oil	863	2048	0.1404	0.00007
MoS$_2$	5.06×10^3	397.21	904.4	2.8424

Table 1. Numerical values of thermophysical properties.

where ϕ describes the volume fraction of nanoparticles. The subscripts s and f stands for solid nanoparticles and base fluid, respectively. The numerical values of physical properties of nanoparticle and base fluid are mentioned in **Table 1**.

Introducing the following dimensional less variables

$$v = \frac{u}{U}, \quad \xi = \frac{U}{v}y, \quad \tau = \frac{U^2}{v}t, \quad \theta = \frac{T - T_\infty}{T_w - T_\infty}, \quad \Phi = \frac{C - C_\infty}{C_w - C_\infty}.$$

into Eqs. (1)–(4), we get

$$\frac{\partial v}{\partial \tau} = \frac{1}{Re}\frac{\partial^2 v}{\partial \xi^2} + \frac{\beta}{a_1}\frac{\partial^3 v}{\partial \tau \partial \xi^2} - M_1 v + Gr\phi_2\theta + Gm\phi_3\Phi, \tag{5}$$

$$\frac{Pr\phi_4}{\lambda_{nf}}\frac{\partial \theta}{\partial \tau} = \frac{\partial^2 \theta}{\partial \xi^2}, \tag{6}$$

$$\frac{\partial \Phi}{\partial \tau} = \frac{1}{a_4}\frac{\partial^2 \Phi}{\partial \xi^2}. \tag{7}$$

$$
\begin{array}{lll}
v(\xi, 0) = 0 & \theta(\xi, 0) = 0 & \Phi(\xi, 0) = 0 \\
v(0, \tau) = \cos \omega\tau & \theta(0, \tau) = 1 & \Phi(0, \tau) = 1 \\
v(\infty, \tau) = 0 & \theta(\infty, \tau) = 0 & \Phi(\infty, \tau) = 0,
\end{array}
\tag{8}
$$

where

$$Re = (1 - \phi)^{2.5}a_1, \qquad M_1 = \frac{M\phi_1}{a_1}, \qquad \phi_1 = 1 + \frac{3(\sigma - 1)\phi}{(\sigma + 2) - (\sigma - 1)},$$

$$\phi_2 = (1 - \phi)\rho_f + \phi\rho_s\frac{\beta_{Ts}}{\beta_{Tf}}, \qquad \phi_3 = (1 - \phi)\rho_f + \phi\rho_s\frac{\beta_{Cs}}{\beta_{Cf}},$$

$$\phi_4 = (1 - \phi) + \phi\frac{(\rho c_p)_s}{(\rho c_p)_f}, \qquad \lambda_{nf} = \frac{k_{nf}}{k_f}, \qquad a_1 = (1 - \phi) + \phi\frac{\rho_s}{\rho_f}, \qquad a_4 = \frac{Sc}{(1 - \phi)},$$

where Re is the Reynolds number, $\beta = \frac{\alpha_1 U^2}{\rho_f v^2}$ is the non-dimensional second-grade parameter,

$M = \frac{\sigma_f B_0^2 v}{\rho_f U^2}$ shows the Hartmann number (magnetic parameter), $Gr = \frac{g v \beta_{Tf}}{U^3}(T_w - T_\infty)$ is the

thermal Grashof number, $Gm = \frac{g\nu\beta_{Cf}}{U^3}(C_w - C_\infty)$ is the mass Grashof number, $\mathrm{Pr} = \frac{(\mu c_p)_f}{k}$ is the Prandtl number and $Sc = \frac{\nu}{D_f}$ is the Schmidt number.

3. Exact solution

In order to develop the generalized second-grade nanofluid model, we replace the partial derivative with respect to τ by CF fractional operator of order α, and Eqs. (5)–(7) can be written as

$$D_\tau^\alpha v(\xi, \tau) = \frac{1}{\mathrm{Re}}\frac{\partial^2 v}{\partial \xi^2} + \frac{\beta}{a_1}D_\tau^\alpha \frac{\partial^3 v}{\partial \tau \partial \xi^2} - M_1 v + Gr\phi_2\theta + Gm\phi_3\Phi, \tag{9}$$

$$\frac{\mathrm{Pr}\,\phi_4}{\lambda_{nf}}D_\tau^\alpha\theta = \frac{\partial^2\theta}{\partial\xi^2}, \tag{10}$$

$$a_4 D_\tau^\alpha \Phi = \frac{\partial^2\Phi}{\partial\xi^2}, \tag{11}$$

where D_τ^α (.) is known as Caputo-Fabrizio time fractional operator and is defined as:

$$D_\tau^\alpha f(\tau) = \frac{1}{1-\alpha}\int_0^\tau \exp\left(\frac{-\alpha(\tau - t)}{1-\alpha}\right)f''(\tau)dt; \qquad \text{for} \quad 0 < \alpha < 1 \tag{12}$$

Applying Laplace transform to Eqs. (9)–(11) and using the corresponding initial conditions from Eq. (8), we have:

$$\frac{d^2\overline{\theta}(\xi, q)}{d\xi^2} - \frac{b_1 q}{q + \gamma_1}\overline{\theta}(\xi, q) = 0, \tag{13}$$

$$\frac{d^2\overline{\Phi}(\xi, q)}{d\xi^2} - \frac{a_2 q}{q + \gamma_1}\overline{\Phi}(\xi, q) = 0, \tag{14}$$

$$\frac{d^2\overline{v}(\xi, q)}{d\xi^2} - \frac{M_4(q + M_3)}{(q + d_1)}\overline{v}(\xi, q) = -Gr\phi_2\overline{\theta}(\xi, q) - Gm\phi_3\overline{\Phi}(\xi, q). \tag{15}$$

where $b_1 = \frac{\mathrm{Pr}\phi_4}{\lambda_{nf}}\gamma_0$, $\gamma_1 = \alpha\gamma_0$, $a_2 = a_4\gamma_0$, $M_4 = \frac{M_1 + \gamma_0}{d_0}$, $M_3 = \frac{M_1\gamma_1}{M_1 + \gamma_0}$, $d_1 = \frac{a_1\gamma_1}{a_1 + \mathrm{Re}\beta\gamma_0}$, $\gamma_0 = \frac{1}{1-\alpha}$ and $d_0 = \frac{a_1 + \mathrm{Re}\beta\gamma_0}{\mathrm{Re}a_1}$.

Boundary conditions are transformed to:

$$\overline{\theta}(0, q) = \frac{1}{q}, \quad \overline{\theta}(\infty, q) = 0, \tag{16}$$

$$\overline{\Phi}(0, q) = \frac{1}{q}, \quad \overline{\Phi}(\infty, q) = 0, \tag{17}$$

$$\overline{v}(0,q) = \frac{q}{q^2 + \omega^2}, \quad \overline{v}(\infty, q) = 0. \tag{18}$$

Upon solving Eqs. (13)–(15) and using the boundary conditions from Eqs. (16)–(18), we get:

$$\overline{\theta}(\xi, q) = \frac{1}{q}\exp\left(-\xi\sqrt{\frac{b_1 q}{q + \gamma_1}}\right), \tag{19}$$

$$\overline{\Phi}(\xi, q) = \frac{1}{q}\exp\left(-\xi\sqrt{\frac{a_2 q}{q + \gamma_1}}\right), \tag{20}$$

$$\begin{aligned}
\overline{v}(\xi, q) = &\frac{1}{2}\overline{\chi}\left(\xi\sqrt{M_4}, q, -i\omega, M_3, d_1\right) + \frac{1}{2}\overline{\chi}\left(\xi\sqrt{M_4}, q, i\omega, M_3, d_1\right) \\
&+ Gr_3\overline{\chi}\left(\xi\sqrt{M_4}, q, 0, M_3, d_1\right) + R_0\overline{\chi}\left(\xi\sqrt{M_4}, q, d_2, M_3, d_1\right) \\
&+ R_1\overline{\chi}\left(\xi\sqrt{M_4}, q, d_3, M_3, d_1\right) + Gm_3\overline{\chi}\left(\xi\sqrt{M_4}, q, 0, M_3, d_1\right) \\
&+ R_2\overline{\chi}\left(\xi\sqrt{M_4}, q, d_4, M_3, d_1\right) + R_3\overline{\chi}\left(\xi\sqrt{M_4}, q, d_5, M_3, d_1\right) \\
&- Gr_3\overline{\chi}\left(\xi\sqrt{b_1}, q, 0, 0, \gamma_1\right) - R_0\overline{\chi}\left(\xi\sqrt{b_1}, q, d_2, 0, \gamma_1\right) \\
&- R_1\overline{\chi}\left(\xi\sqrt{b_1}, q, d_3, 0, \gamma_1\right) - Gm_3\overline{\chi}\left(\xi\sqrt{a_2}, q, 0, 0, d_1\right) \\
&- R_2\overline{\chi}\left(\xi\sqrt{a_2}, q, d_4, 0, d_1\right) - R_3\overline{\chi}\left(\xi\sqrt{a_2}, q, d_5, 0, d_1\right),
\end{aligned} \tag{21}$$

$$\overline{\chi}(\xi, q, a, b, c) = \frac{1}{q + a}\exp\left(-\xi\sqrt{\frac{q + b}{q + c}}\right). \tag{22}$$

Eqs. (19) and (20) are written in simplified form

$$\overline{\theta}(\xi, q) = \overline{\chi}\left(\xi\sqrt{b_1}, q, 0, 0, \gamma_1\right), \tag{23}$$

$$\overline{\Phi}(\xi, q) = \overline{\chi}\left(\xi\sqrt{a_2}, q, 0, 0, \gamma_1\right), \tag{24}$$

where

$$Gr_3 = \frac{Gr_2\gamma_1^2}{d_2 d_3}, \quad Gm_3 = \frac{Gm_2\gamma_1^2}{d_4 d_5}, \quad Gr_2 = \frac{Gr_1}{\delta_1}, \quad Gm_2 = \frac{Gm_1}{\delta_6}, \quad R_0 = \frac{-d_2^2 Gr_2 + 2d_2 Gr_2\gamma_1 - Gr_2\gamma_1^2}{d_2 - d_3},$$

$$R_1 = \frac{-d_3^2 Gr_2 - 3d_3 Gr_2\gamma_1 + Gr_2\gamma_1^2}{d_2 - d_3}, \quad R_2 = \frac{-d_4^2 Gm_2 + 2d_4 Gm_2\gamma_1 - Gm_2\gamma_1^2}{d_4 - d_5},$$

$$R_3 = \frac{d_5^2 Gm_2 - 3d_5 Gm_2\gamma_1 + Gm_2\gamma_1^2}{d_4 - d_5}, \quad d_2 = \frac{\delta_4}{2} + \sqrt{\frac{\delta_4^2 + 4\delta_5}{2}}, \quad d_3 = \frac{\delta_4}{2} - \sqrt{\frac{\delta_4^2 + 4\delta_5}{2}},$$

$$d_4 = \frac{\delta_8}{2} + \sqrt{\frac{\delta_8^2 + 4\delta_9}{2}}, \quad d_5 = \frac{\delta_8}{2} - \sqrt{\frac{\delta_8^2 + 4\delta_9}{2}}, \quad Gr_1 = \frac{Gr\phi_2}{d_0}, \quad Gm_1 = \frac{Gm\phi_3}{d_0}, \quad \delta_1 = b_1 M_4,$$

$$\delta_2 = b_1 d_1 - M_4 \gamma_1 - M_4 M_3, \quad \delta_3 = M_4 M_3 \gamma_1, \quad \delta_4 = \frac{\delta_2}{\delta_1}, \quad \delta_5 = \frac{\delta_3}{\delta_1}, \quad \delta_6 = a_2 - M_4,$$

$$\delta_7 = a_2 d_1 - M_4 \gamma_1 - M_4 M_3, \quad \delta_8 = \frac{\delta_7}{\delta_6}, \quad \delta_9 = \frac{\delta_3}{\delta_6}.$$

Now, inverse Laplace transform of Eqs. (21), (23) and (24) is:

$$
\begin{aligned}
v(\xi, \tau) = & \frac{1}{2} \chi\left(\xi\sqrt{M_4}, \quad \tau, -i\omega, \quad M_3, \quad d_1\right) + \frac{1}{2}\chi\left(\xi\sqrt{M_4}, \tau, i\omega, M_3, d_1\right) \\
& + Gr_3 \chi\left(\xi\sqrt{M_4}, \tau, 0, M_3, d_1\right) + R_0 \chi\left(\xi\sqrt{M_4}, \tau, d_2, M_3, d_1\right) \\
& + R_1 \chi\left(\xi\sqrt{M_4}, \tau, d_3, M_3, d_1\right) + Gm_3 \chi\left(\xi\sqrt{M_4}, \tau, 0, M_3, d_1\right) \\
& + R_2 \chi\left(\xi\sqrt{M_4}, \tau, d_4, M_3, d_1\right) + R_3 \chi\left(\xi\sqrt{M_4}, \tau, d_5, M_3, d_1\right) - Gr_3 \chi\left(\xi\sqrt{b_1}, \tau, 0, 0, \alpha\gamma_0\right) \\
& - R_0 \chi\left(\xi\sqrt{b_1}, \tau, d_2, 0, \alpha\gamma_0\right) - R_1 \chi\left(\xi\sqrt{b_1}, \tau, d_3, 0, \alpha\gamma_0\right) - Gm_3 \chi(\xi\sqrt{a_2}, \tau, 0, 0, d_1) \\
& - R_2 \chi(\xi\sqrt{a_2}, \tau, d, 0, d_1) - R_3 \chi(\xi\sqrt{a_2}, \tau, d_5, 0, d_1),
\end{aligned}
\tag{25}
$$

$$\theta(\xi, \tau) = \chi\left(\xi\sqrt{b_1}, \tau, 0, 0, \gamma_1\right), \tag{26}$$

$$\Phi(\xi, \tau) = \chi\left(\xi\sqrt{a_2}, \tau, 0, 0, \gamma_1\right), \tag{27}$$

where

$$\overline{\chi}(\xi, q; a, b, c) = \frac{1}{q+a}\exp\left(-\xi\sqrt{\frac{q+b}{q+c}}\right), \tag{28}$$

$$\chi(\xi, \tau, a, b, c) = e^{-a\tau - \xi} - \frac{\xi\sqrt{b-c}}{2\sqrt{\pi}}\int_0^\infty\int_0^\tau \frac{e^{a\tau}}{\sqrt{\tau}}\exp\left(a\tau - c\tau - \frac{\xi^2}{4u} - u\right)I_1\left(2\sqrt{(b-c)ut}\right)dtdu. \tag{29}$$

Skin friction, Nusselt number and Sherwood number.

Skin friction, Nusselt number and Sherwood number are defined as:

$$C_f = \frac{1}{(1-\phi)^{2.5}}\frac{\partial v}{\partial \xi} + \beta \frac{\partial^2 v}{\partial \xi \partial \tau}\bigg|_{\xi=0}, \tag{30}$$

$$Nu = \frac{\partial \theta}{\partial \xi}\bigg|_{\xi=0}, \tag{31}$$

$$Sh = \frac{\partial \Phi}{\partial \xi}\bigg|_{\xi=0}. \tag{32}$$

Velocity field for regular grade-two fluid without mass transfer.

For $Gm = \phi = 0$ in Eq. (22) reduce to the following form:

$$v(\xi, \tau) = \frac{1}{2}\chi\left(\xi\sqrt{M_4}, \ \tau, -i\omega, \ M_3, \ d_1\right) + \frac{1}{2}\chi\left(\xi\sqrt{M_4}, \tau, i\omega, M_3, d_1\right) + Gr_3\chi\left(\xi\sqrt{M_4}, \tau, 0 \ , M_3, d_1\right)$$
$$+ R_0\chi\left(\xi\sqrt{M_4}, \tau, \ d_2, M_3, d_1\right) + R_1\chi\left(\xi\sqrt{M_4}, \tau, d_3, M_3, d_1\right) - Gr_3\chi\left(\xi\sqrt{b_1}, \tau, 0, 0, \alpha\gamma_0\right) \tag{33}$$
$$- R_0\chi\left(\xi\sqrt{b_1}, \tau, d_2, 0, \alpha\gamma_0\right) - R_1\chi\left(\xi\sqrt{b_1}, \tau, d_3, 0, \alpha\gamma_0\right),$$

where $b_1 = \Pr\gamma_0$, $M_4 = \frac{M+\gamma_0}{d_0}$, $M_3 = \frac{M\gamma_1}{M+\gamma_0}$, $d_1 = \frac{\gamma_1}{d_0}$, $d_0 = 1 + \beta\gamma_0$, $Gr_1 = \frac{Gr}{d_0}$,

which is quite identical to the solution of Sheikh et al. [19] for $\frac{1}{k} = R = 0$.
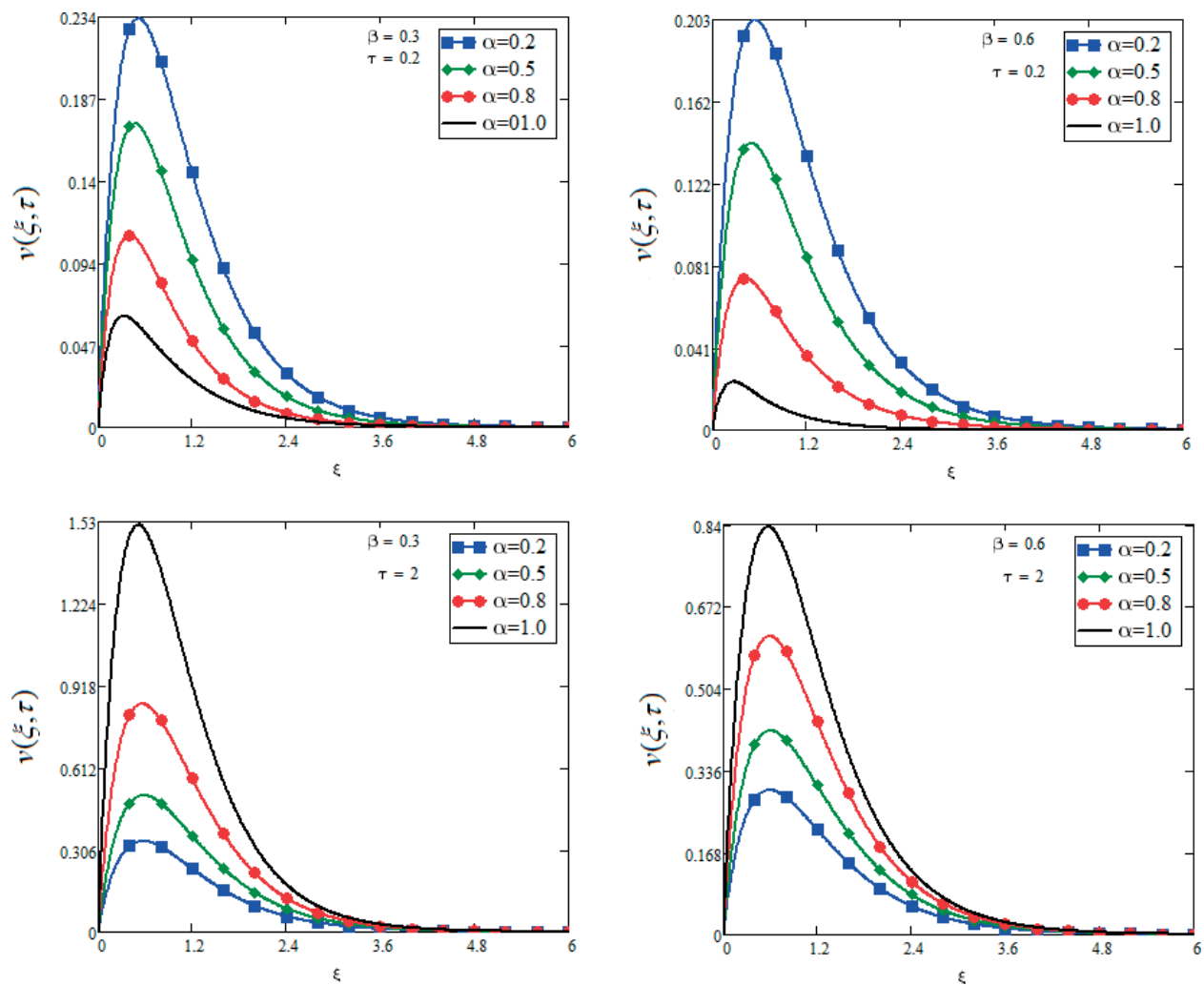

Figure 2. Velocity profile for different values of β when $M = 1$, $Gr = Gm = 2$, $\Pr = 5$, $Sc = 5$ and $\phi = 0.02$.

4. Graphical discussion

A fractional model for the outflow of the second-grade fluid with nanoparticles over an isothermal vertical plate is studied. The coupled partial differential equations with Caputo-Fabrizio time-fractional derivatives are solved analytically via Laplace transform method. Furthermore, the influence of different embedded parameters such as α, ϕ, β, M, t Gr, Gm and Sc is shown graphically.

Figures 2–7 depict the effect of α on $v(\xi, \tau)$ for two different values of time. It is clear from the figures that for smaller value of τ, when ($\tau = 0.2$) fractional velocity is larger than classical velocity and for larger value of τ, when ($\tau = 2$) fractional velocity is less than classical velocity. Clearly, increasing values of α decrease $v(\xi, \tau)$.

Figure 2 represents the influence of β on both the velocity and microrotation profiles. A decreasing behaviour is observed for increasing values of β in both cases. In this figure, the comparison of second-grade fluid velocity with Newtonian fluid velocity is plotted. It is
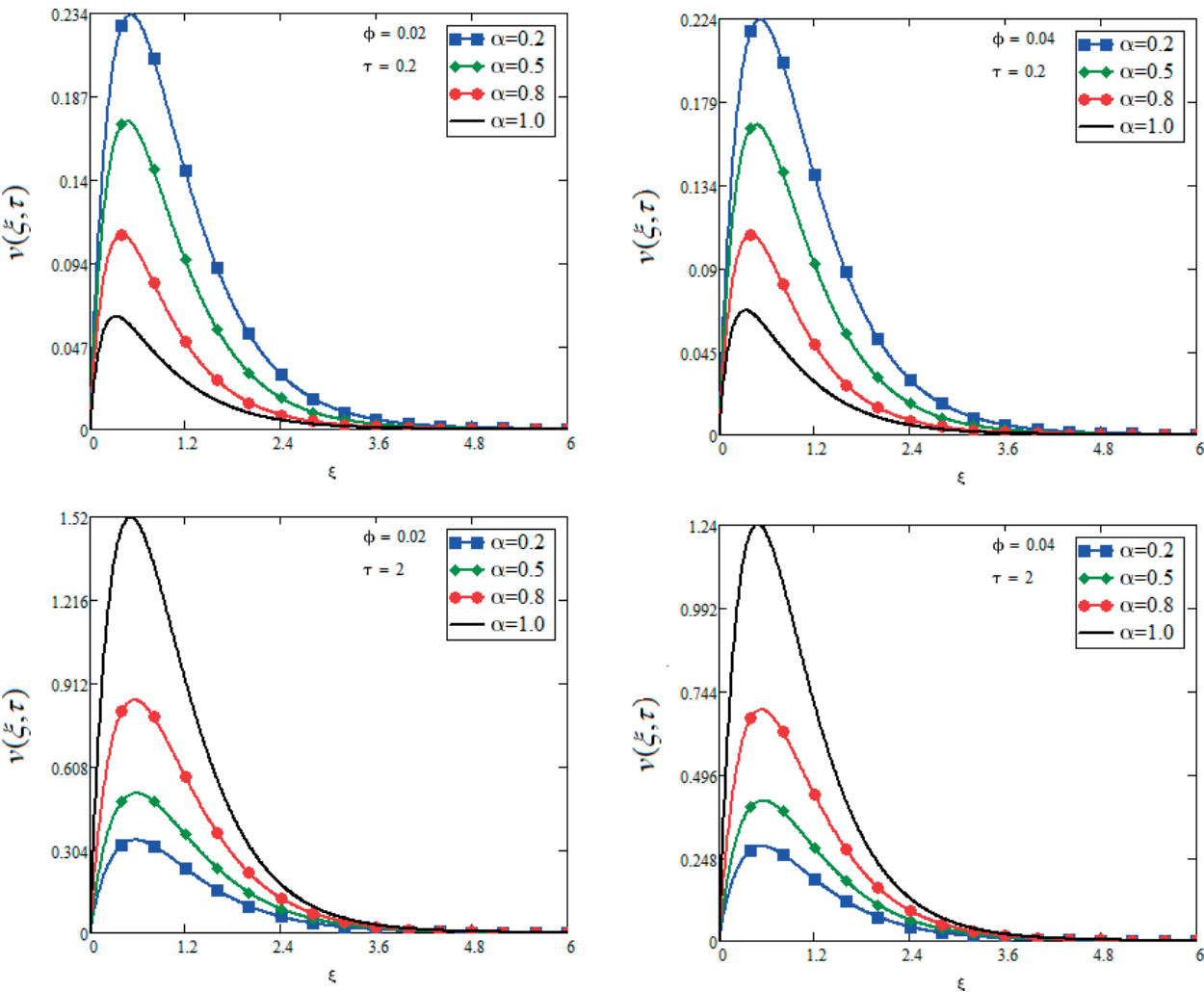

Figure 3. Velocity profile for different values of ϕ when $M = 1, Gr = Gm = 2, \Pr = 5, Sc = 5 \; and \; \beta = 0.3$.
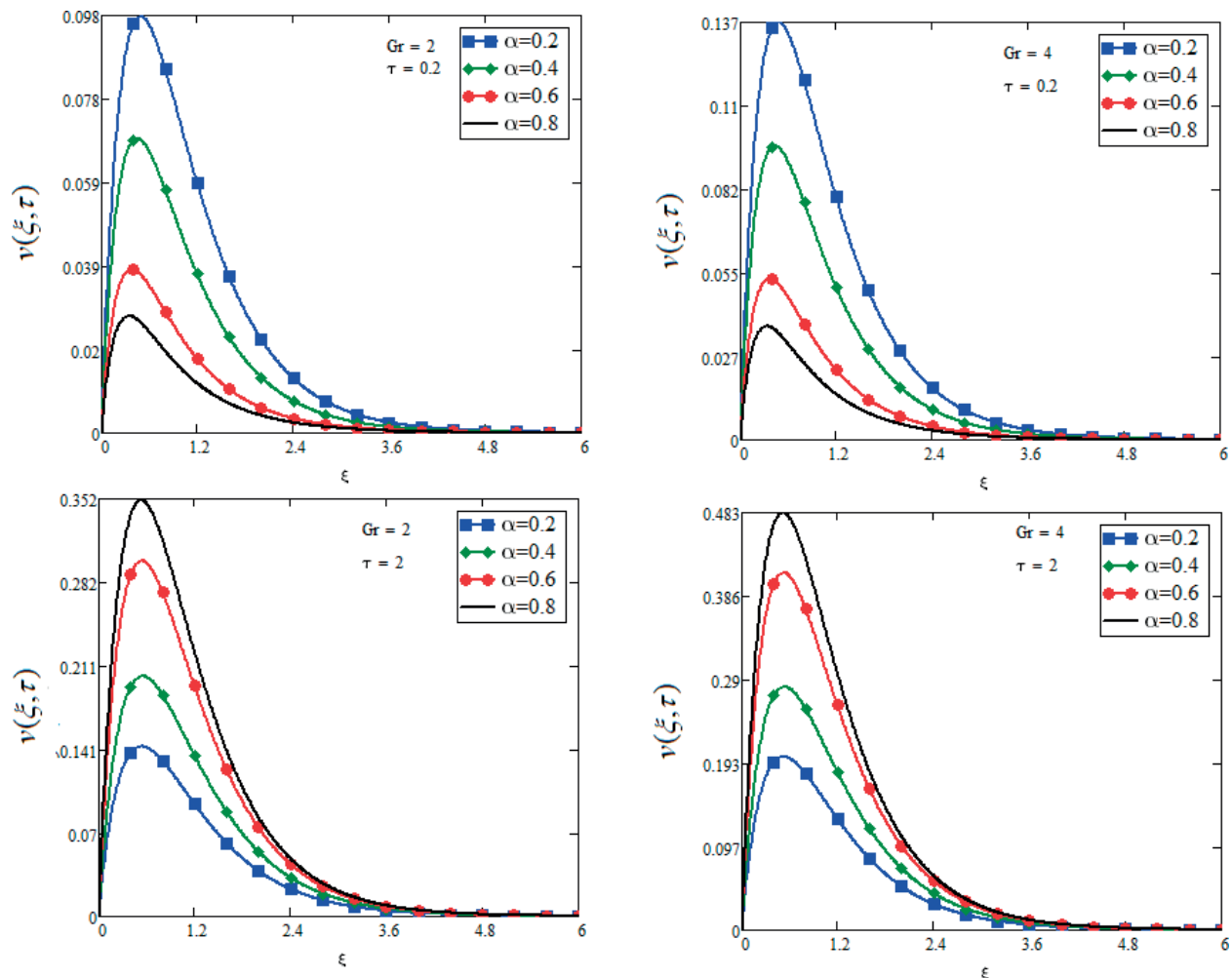
Figure 4. Velocity profile for different values of Gr when $M = 1, \phi = 0.02, Gm = 2, \Pr = 5, Sc = 5$ *and* $\beta = 0.3$.

obvious that the boundary layer thickness of second-grade fluid velocity is greater as compared to boundary layer thickness of Newtonian fluid. More clearly, the velocity of second-grade fluid is smaller than Newtonian fluid.

Figure 3 shows the influence of ϕ on the flow. It was found that the velocity of fluid decreases with the increase in ϕ due to the increase in viscosity. Because by increasing volume fraction, the fluid becomes more viscous, which leads to a decrease in the fluid velocity.

Figures 4 and **5** show the influence of thermal Grashof number Gr and mass Grashof number Gm on velocity and microrotation. Increasing values of both of these parameters are responsible for the rise in buoyancy forces and reducing viscous forces, which result in an increase in fluid velocity and magnitude of microrotation.

Figure 6 depicts the MHD effect on velocity. In this type of flows, magnetic force results in achieving steady state much faster than the non-MHD flows. Moreover, increasing values of M enhances the Lorentz forces, as a result decelerates the fluid velocity. **Figure 7** illustrates variations in velocity for different values of Schmidt number, Sc. It shows that velocity decreases
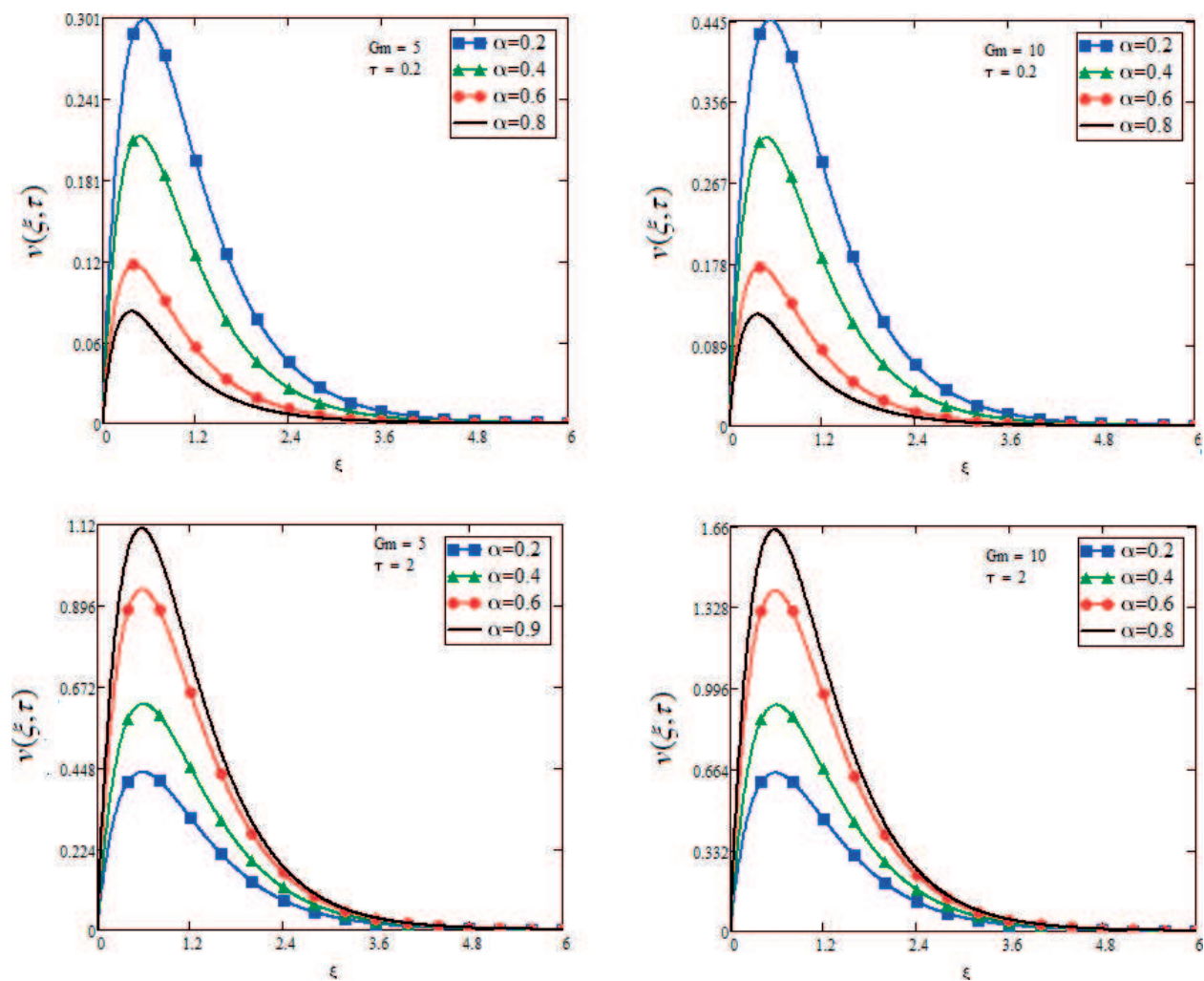
Figure 5. Velocity profile for different values of *Gm* when $M = 1, Gr = 2, \phi = 0.02, \Pr = 5, Sc = 5$ and $\beta = 0.3$.

when *Sc* value increases. The effect of Schmidt number on velocity is identical to that of the magnetic parameter. The influence of phase angle $\omega\tau$ on the velocity profile is shown in **Figure 8**. The velocity is showing fluctuating behaviour.

In order to show the effect of α, τ *and* ϕ on the temperature profile in **Figure 9**, it is found that temperature increasing with increasing value of ϕ. **Figure 10** shows the effect of α and τ on temperature profile. This figure shows the effect of α on the temperature profile for two different values of τ. For smaller value of τ ($\tau = 0.2$), classical temperature is less than fractional temperature, and for larger value, when $\tau = 2$, then the graph shows opposite behaviour. **Figure 11** shows the comparison of present solution with published result of Sheikh et al. [19]. It is noted that in the absence of porosity and radiation, the present result is similar to those obtained in [19. See **Figure 9**], which shows the validity of our obtained results.

Variations in skin friction, Nusselt number and Sherwood number are shown in **Tables 2–4**. The effect of β, α, *Gr, Gm, M, Sc*, ϕ, $\omega\tau$ *and* τ on the skin friction is studied in **Table 2**. It is found
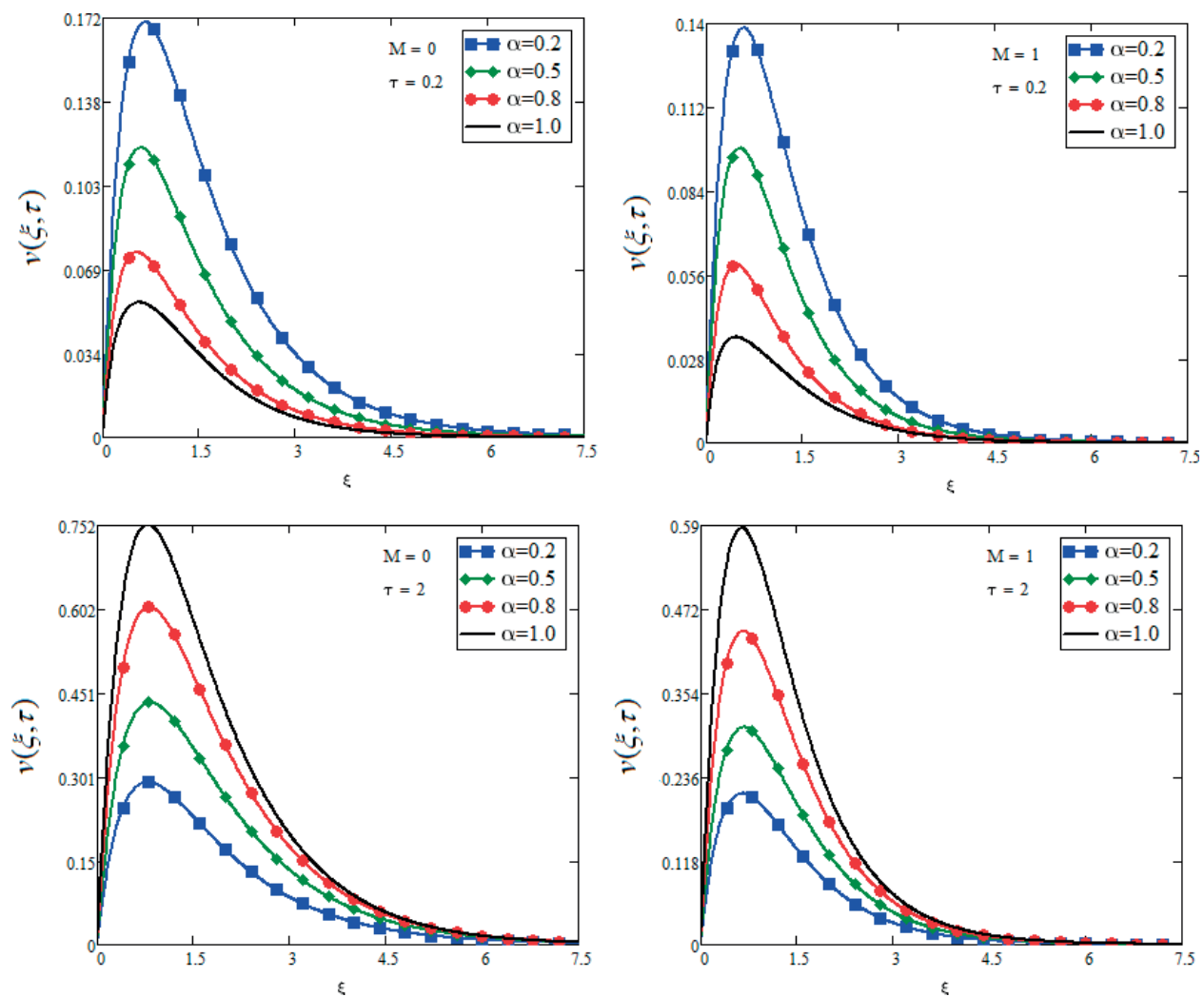
Figure 6. Velocity profile for different values of M when $\phi = 0.02, Gr = Gm = 2, \Pr = 5, Sc = 5$ and $\beta = 0.3$.

that skin friction increases when there is an increase in $\alpha, Gr, Gm, M, Sc, \omega\tau$ and τ. but it is noticed that for increasing value of β and ϕ, skin friction decreases. It is due to the fact that when ϕ increases, it gives rise to lubricancy of the oil. **Table 3** represents the effect of α, ϕ and τ on Nusselt number. As values of α, ϕ and τ increase, Nusselt number decreases. From **Table 4**, it is clear that when Sc increases, Sherwood number increases, and an increase in τ decreases Sherwood number.

5. Conclusion remarks

Unsteady MHD flow of generalized second-grade fluid along with nanoparticles has been analyzed. The exact solution has been obtained for velocity, temperature and concentration profile via the Laplace transform technique. The effects of various physical parameters are studied in various plots and tables with the following conclusions:
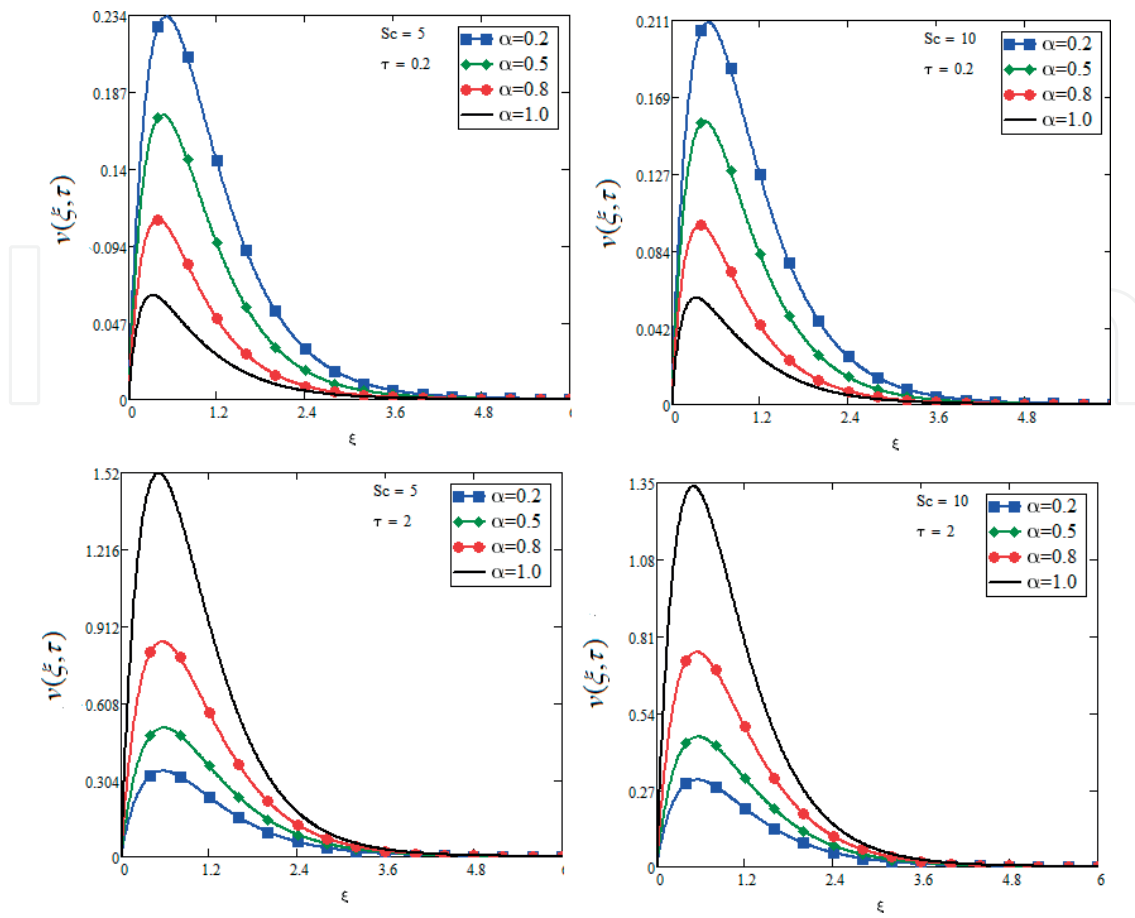
Figure 7. Velocity profile for different values of Sc when $M = 1, Gr = Gm = 2, \Pr = 5, \phi = 0.02$ *and* $\beta = 0.3$.
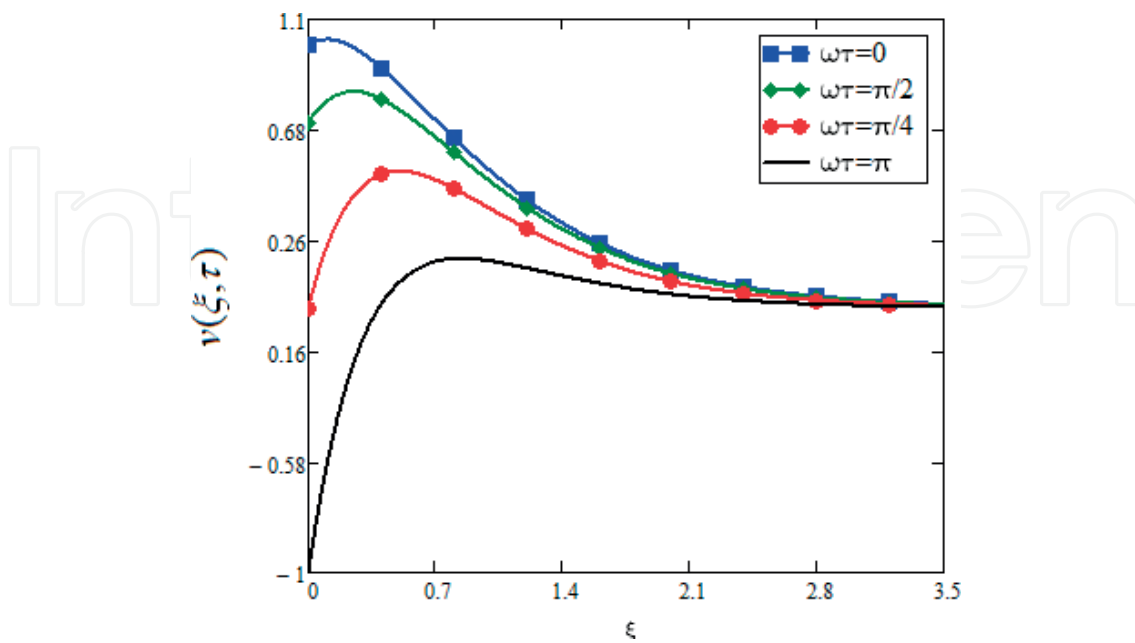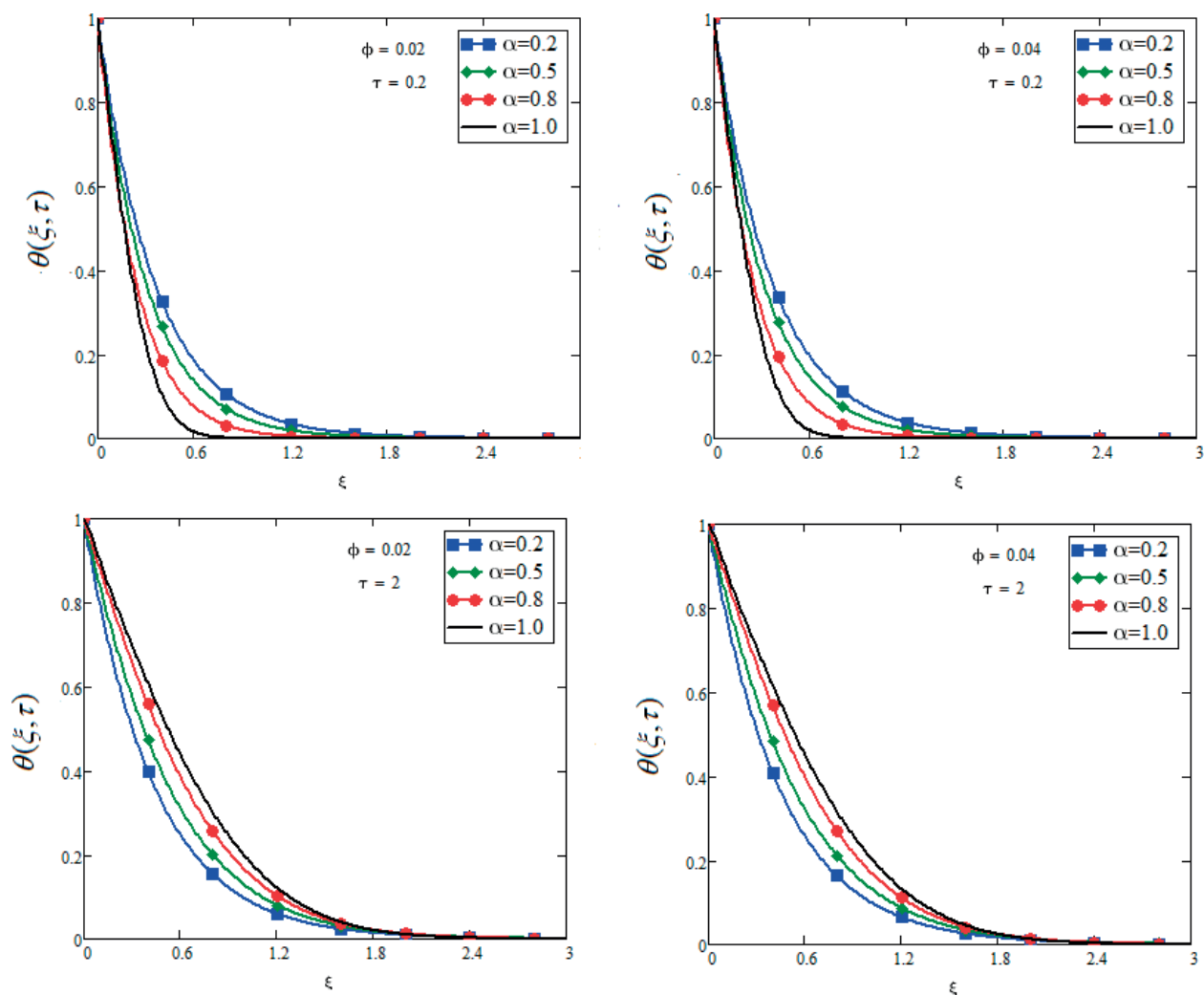

Figure 8. Velocity profile for different values of ω.

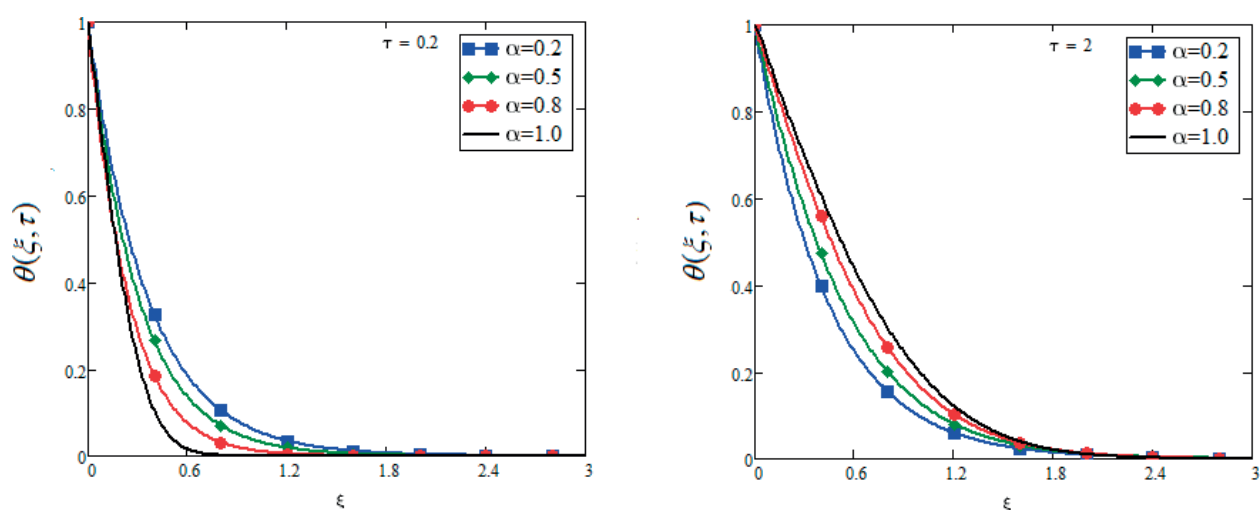**Figure 9.** Temperature profile for different values of ϕ when Pr $= 5$.

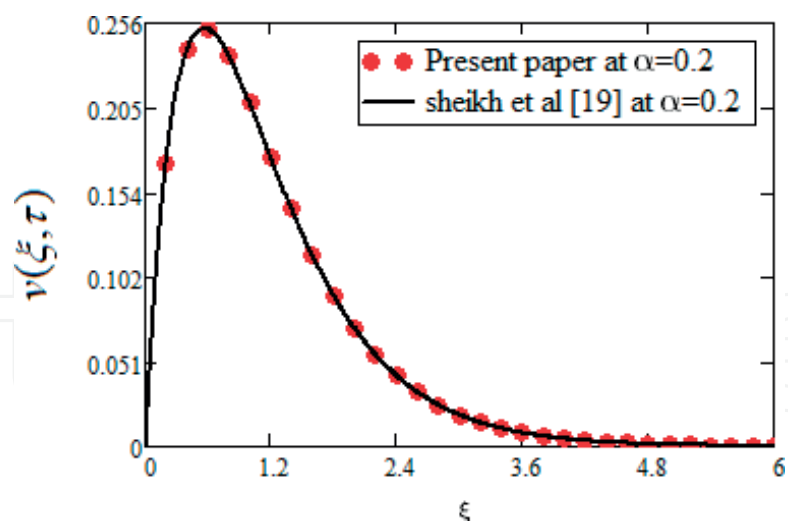**Figure 10.** Temperature profile for different values of time parameter.

Figure 11. Comparison of this study with Sheikh et al. [19], when $\frac{1}{k} = R = 0$.

β	α	Gr	Gm	M	Sc	ϕ	$\omega\tau$	τ	C_f
0.3	0.2	5	5	1	5	0.02	$\frac{\pi}{2}$	2	2.867
$\overline{0.6}$	0.2	5	5	1	5	0.02	$\frac{\pi}{2}$	2	2.857
0.3	$\overline{0.4}$	5	5	1	5	0.02	$\frac{\pi}{2}$	2	3.66
0.3	0.2	$\overline{7}$	5	1	5	0.02	$\frac{\pi}{2}$	2	4.121
0.3	0.2	5	$\overline{\overline{7}}$	1	5	0.02	$\frac{\pi}{2}$	2	4.086
0.3	0.2	5	5	$\overline{2}$	5	0.02	$\frac{\pi}{2}$	2	2.869
0.3	0.2	5	5	1	$\overline{7}$	0.02	$\frac{\pi}{2}$	2	3.135
0.3	0.2	5	5	1	5	$\overline{0.04}$	$\frac{\pi}{2}$	2	0.599
0.3	0.2	5	5	1	5	0.02	$\overline{\pi}$	2	4.371
0.3	0.2	5	5	1	5	0.02	$\frac{\pi}{2}$	$\overline{4}$	3.719

Table 2. Effect of various parameters on the skin friction.

α	ϕ	τ	Nu
0.2	0.02	2	−1.923
$\overline{0.4}$	0.02	2	−1.606
0.2	$\overline{0.04}$	2	−1.872
0.2	0.02	$\overline{4}$	−1.526

Table 3. Effect of various parameters on the Nusselt number.

Sc	τ	Sh
5	2	−2.018
$\overline{7}$	2	−2.388
5	$\overline{4}$	−1.646

Table 4. Effect of various parameters on the Sherwood number.

- With increase in volume friction ϕ of nanofluid, lubricancy of the fluid increases.

- An increase in second-grade parameter β leads to a decrease in fluid velocity.

- The velocity profile shows different behaviour for fractional parameter for different values of time.

- In limited cases, the obtained solutions reduced to the solution of Sheikh et al. [19].

Author details

Farhad Ali[1,2,3]*, Madeha Gohar[3], Ilyas Khan[4], Nadeem Ahmad Sheikh[3], Syed Aftab Alam Jan[3] and Muhammad Saqib[3]

*Address all correspondence to: farhad.ali@tdt.edu.vn

1 Computational Analysis Research Group, Ton Duc Thang University, Ho Chi Minh City, Vietnam

2 Faculty of Mathematics and Statistics, Ton Duc Thang University, Ho Chi Minh City, Vietnam

3 Department of Mathematics, City University of Science and Information Technology, Peshawar, Khyber Pakhtunkhwa, Pakistan

4 Basic Engineering Sciences Department, College of Engineering Majmaah University, Majmaah Saudi Arabia

References

[1] Nonnenmacher TF, Metzler R. On the Riemann-Liouville fractional calculus and some recent applications. Fractals. 1995;**3**(03):557-566

[2] Sabatier J, Agrawal OP, Machado JT. Advances in fractional calculus (Vol. 4, no. 9). Dordrecht: Springer; 2007

[3] Laskin N. Fractional schrödinger equation. Physical Review E. 2002;**66**(5) 056108

[4] Naber M. Time fractional Schrödinger equation. Journal of Mathematical Physics. 2004; **45**(8):3339-3352

[5] Baleanu D, Golmankhaneh AK, Golmankhaneh AK. The dual action of fractional multi time Hamilton equations. International Journal of Theoretical Physics. 2009;**48**(9):2558-2569

[6] Mainardi F. Fractional Calculus and Waves in Linear Viscoelasticity: An Introduction to Mathematical Models. London, UK: World Scientific; 2010

[7] Hayat T, Nadeem S, Asghar S. Periodic unidirectional flows of a viscoelastic fluid with the fractional Maxwell model. Applied Mathematics and Computation. 2004;**151**(1): 153-161

[8] Qi H, Jin H. Unsteady rotating flows of a viscoelastic fluid with the fractional Maxwell model between coaxial cylinders. Acta Mechanica Sinica. 2006;**22**(4):301-305

[9] Meral FC, Royston TJ, Magin R. Fractional calculus in viscoelasticity: An experimental study. Communications in Nonlinear Science and Numerical Simulation. 2010;**15**(4): 939-945

[10] Qi H, Xu M. Unsteady flow of viscoelastic fluid with fractional Maxwell model in a channel. Mechanics Research Communications. 2007;**34**(2):210-212

[11] Carpinteri A, Mainardi F. Fractals and fractional calculus in continuum mechanics (Vol. 378). Verlag GmbH Wien: Spring; 2014

[12] Hilfer R. Threefold introduction to fractional derivatives. Anomalous transport: Foundations and applications. 2008:17-73

[13] Gorenflo R, Mainardi F, Moretti D, Paradisi P. Time fractional diffusion: A discrete random walk approach. Nonlinear Dynamics. 2002;**29**(1):129-143

[14] Ali F, Jan SAA, Khan I, Gohar M, Sheikh NA. Solutions with special functions for time fractional free convection flow of brinkman-type fluid. The European Physical Journal Plus. 2016;**131**(9):310

[15] Shahid N. A study of heat and mass transfer in a fractional MHD flow over an infinite oscillating plate. SpringerPlus. 2015;**4**(1):640

[16] Caputo M, Fabrizio M. A new definition of fractional derivative without singular kernel. Progress in Fractional Differentiation and Applications. 2015;**1**(2):1-13

[17] Shah NA, Khan I. Heat transfer analysis in a second grade fluid over and oscillating vertical plate using fractional Caputo–Fabrizio derivatives. The European Physical Journal C. 2016;**76**(7):1-11

[18] Ali F, Saqib M, Khan I, Sheikh NA. Application of Caputo-Fabrizio derivatives to MHD free convection flow of generalized Walters'-B fluid model. The European Physical Journal Plus. 2016;**131**(10):377

[19] Sheikh NA, Ali F, Khan I, Saqib M. A modern approach of Caputo–Fabrizio time-fractional derivative to MHD free convection flow of generalized second-grade fluid in a porous medium. Neural Computing and Applications. 1-11

[20] Choi SU. Enhancement thermal conductivity of fluids with nanoparticles. International Mechanical Engineering Congress and exposition. 1995

[21] Wu YY, Kao MJ. Using TiO_2 nanofluid additive for engine lubrication oil. Industrial Lubrication and Tribology. 2011;**63**(6):440-445

[22] Wang X, Xu X, Choi S, U S. Thermal conductivity of nanoparticle-fluid mixture. Journal of Thermophysics and Heat Transfer. 1999;**13**(4):474-480

[23] Garg J, Poudel B, Chiesa M, Gordon JB, Ma JJ, Wang JB, et al. Enhanced thermal conductivity and viscosity of copper nanoparticles in ethylene glycol nanofluid. Journal of Applied Physics. 2008;**103**(7):074301

[24] Lee JH, Hwang KS, Jang SP, Lee BH, Kim JH, Choi SU, Choi CJ. Effective viscosities and thermal conductivities of aqueous nanofluids containing low volume concentrations of Al_2O_3 nanoparticles. International Journal of Heat and Mass Transfer. 2008;**51**(11):2651-2656

[25] Abdullah MIHC, Abdollah MFB, Amiruddin H, Nuri M, Rashid N. Effect of hBN/Al_2O_3 nanoparticle additives on the tribological performance of engine oil. Jurnal Teknologi. 2014;**66**(3):1-6

[26] Winer WO. Molybdenum disulfide as a lubricant: A review of the fundamental knowledge. Wear. 1967;**10**(6):422-452

[27] Shafie S, Gul A, Khan I. Molybdenum disulfide nanoparticles suspended in water-based nanofluids with mixed convection and flow inside a channel filled with saturated porous medium. AIP Conference Proceedings. 2016, October;**1775**:030042